

---

VARIOUS TECHNOLOGICAL  
PROCESSES

---

## Hybrid Catalysts Based on Sulfated Zirconium Dioxide and H-beta Zeolite for Alkylation of Isobutane with Isobutylene

E. A. Yuferova\*, S. Yu. Devyatkov, S. P. Fedorov, K. V. Semikin,  
D. A. Sladkovskii, and N. V. Kuzichkin

*St. Petersburg State Technological Institute (Technical University), Moskovskii pr. 26, St. Petersburg, 190013 Russia*  
\*e-mail: Y\_katryn@mail.ru

Received October 31, 2017

**Abstract**—Physicochemical properties of new hybrid catalysts based on sulfated zirconium oxide supported by zeolite of the Beta structural type were studied. The acid-base characteristics of the catalysts are determined by the amount of the supported component, the maximum concentration of Brønsted acid centers ( $277 \mu\text{mol g}^{-1}$ ) is reached upon deposition of 1.7 wt % sulfated zirconium oxide. The texture characteristics of the final catalyst are determined by the starting support. Tests of the catalysts in the reaction of isobutane alkylation with isobutylene demonstrated their advantage in selectivity and stability over the classical bulk sulfated zirconium oxide.

**DOI:** 10.1134/S1070427217100081

New international and domestic gasoline regulations (Euro-4, 5; MSAT II) contain severe saturated vapor pressure constraints and strongly restrict the content of benzene, aromatic hydrocarbons, olefin hydrocarbons, and sulfur, which requires that high-octane nonaromatic components should be added to gasoline.

One of ways to produce components of this kind is by alkylation of isobutane with butylenes. The alkylate (target product of this process) has a low saturated vapor pressure and contains no sulfur, oxygen, nitrogen, and aromatic compounds.

At present isobutane is alkylated with olefins, with the role of catalysts played by sulfuric and hydrofluoric acids and also by mixtures of these with addition of other acids.

Both processes have good parameters as regards the yield, selectivity, and quality of alkylates. However, the application of liquid-acid (homogeneous) catalysts is, first, complicated by their high specific expenditure, toxicity, and corrosion activity and necessary separation of the catalyst-product mixture and the subsequent utilization of spent acids and, second, is hazardous for the health of the operating personnel.

At present, the development of the industrial alkylation is primarily associated with passing from

liquid acids to solid catalysts, which will avoid the above-mentioned problems and gain technological and economical advantages.

In the last decades, there have appeared a number of publications concerned with anion-promoted metal oxides, such as sulfated or tungstic oxides of zirconium, titanium, and aluminum [1]. These catalysts have a specific surface area of 50 to  $180 \text{ m}^2 \text{ g}^{-1}$  and strength of acid centers exceeding that of 100% sulfuric acid. Sulfated zirconium dioxide (SZ) is mostly used in the hydroisomerization of alkanes, which occurs at a substantially lower temperature and does so with higher selectivity, compared with zeolites.

One of ways to modify sulfate-zirconium catalysts is by their deposition onto large-surface-area mesostructured materials having no acidity (e.g., SBA-15) [2]. Deposition of sulfated zirconium dioxide onto the surface of zeolites originally having acid centers may give rise to two types of acid centers that can be simultaneously involved in various catalytic cycles. Examples of such systems were described in [3], where zirconium dioxide was simultaneously promoted with tungsten trioxide  $\text{WO}_3$  and sulfate anions  $\text{SO}_4^{2-}$ . These systems, named hybrid catalysts in the literature [4], possess characteristics that

can exhibit a certain synergism and can even exhibit new properties that are not simply a sum of the properties of the starting components.

The main problem consists in that only a little progress in the development of heterogeneous alkylation catalysts has been made during the recent years because all these catalysts are rapidly deactivated and show a poor selectivity with respect to the target products.

The goal of our study was to examine the physico-chemical characteristics of catalysts having the form of sulfated zirconium dioxide supported by H-Beta zeolite and their effect on the stability and activity in the target reaction of isobutane alkylation with isobutylene.

## EXPERIMENTAL

H-Beta zeolite with Si/Al = 25 was produced by the method described in [5]. Pseudoboehmite of Pural SB brand was used as a binder for catalysts. Zirconium oxychloride (Sigma Aldrich) served as the precursor of zirconium oxide. Sulfate zirconium hydroxide was produced by the method described in [6]: 85 g of concentrated sulfuric acid, 277 mL of deionized water, and 970 g of zirconium oxychloride octahydrate were mixed, and the mixture was cooled to 10°C. Further, a 10% solution of ammonium hydroxide was added under permanent agitation to until pH 12–13 was reached. On being formed, the precipitate was washed until no  $\text{Cl}^-$  and  $\text{SO}_4^{2-}$  ions were found in washing water. On being washed, the precipitate was repeatedly humidified to a moisture content of about 50 wt % and then was subjected to a hydrothermal treatment for 5 h under an excess pressure of approximately 1.5 atm. After the hydrothermal treatment, the precipitate was humidified with a twofold, relative to its mass, amount of deionized water, and concentrated sulfuric acid was added to the resulting suspension (8 wt %  $\text{SO}_4^{2-}$  ions relative to zirconium oxide). After the acid was added, the suspension was agitated 30 min and then dried at 100°C until the whole amount of moisture was removed. After the drying, an additional treatment with sulfuric acid (to additionally introduce 6 wt % sulfo groups) was performed by the method of incipient wetness impregnation.

The molding compound was produced by mixing of a twice sulfated zirconium hydroxide with a calculated amount of pseudoboehmite in a 75 : 25 ratio (calculated for calcined materials) in an excess amount of deionized water. The suspensions were agitated for 1 h and then

dried until the optimal molding moisture content was reached. The materials obtained were molded with a manual extrusion device of piston type with channel diameter of 1.5 mm and dried for 12 h at room temperature and then for 3 h at a temperature of 110°C, with the subsequent calcination at 700°C.

Zeolite of the H-Beta structural type was preliminarily calcined at 300°C for 1 h and then a calculated amount of zirconium dioxide was deposited by the full moisture absorption method from an aqueous solution of  $\text{ZrOCl}_2$ . The resulting samples contained 4, 8, and 16 wt % zirconium dioxide. After the samples were dried at a temperature of 110°C for 3 h, zirconium oxychloride was hydrolyzed in an excess amount of distilled water. Ammonium hydroxide was added dropwise under thorough agitation until the pH reached a value of 11. Then the samples were filtered and washed with an excess of twice-distilled water until  $\text{Cl}^-$  anions disappeared (controlled by  $\text{AgNO}_3$  test), with the subsequent drying at 110°C for 3 g. The sulfation was performed by impregnation by the incipient wetness impregnation method with a sulfuric acid solution (8 wt %  $\text{SO}_3$  relative to zirconium dioxide). The samples were dried at a temperature of 80°C and calcined at 700°C.

To examine the activity, the materials synthesized, which contained zeolite and zirconium dioxide deposited onto the zeolite in amounts of 4, 8, and 16 wt %, were shaped together with Pural SB (Sasol) pseudoboehmite as a binder into extrudates (25 wt % binder in the calcined base). The extrudates were dried at 80°C and calcined at 700°C for 4 h. Prior to the catalytic tests, the catalysts were ground, sieved to obtain a 0.5–1-mm fraction and again calcined at 350°C for 1 h. All the samples are described in Table 1.

The acid centers were quantitatively determined by IR spectroscopy of adsorbed pyridine with a Shimadzu IR Tracer-100 FT-IR spectrometer having an attached vacuum gas cell [7]. Pyridine was desorbed at temperatures of 150, 250, and 350°C. The molar extinction coefficients for Lewis and Brønsted acid centers were taken from the literature [8].

The phase compositions were examined by X-ray diffraction (XRD) analysis on a Shimadzu XRD-7000 instrument with monochromatic  $\text{CuK}_\alpha$  radiation ( $\lambda = 0.154051$  nm).

The texture characteristics were determined with a Quantachrome Autosorb-6 ISA specific surface area analyzer. Nitrogen gas served as adsorbate, the

**Table 1.** Description of the catalysts synthesized

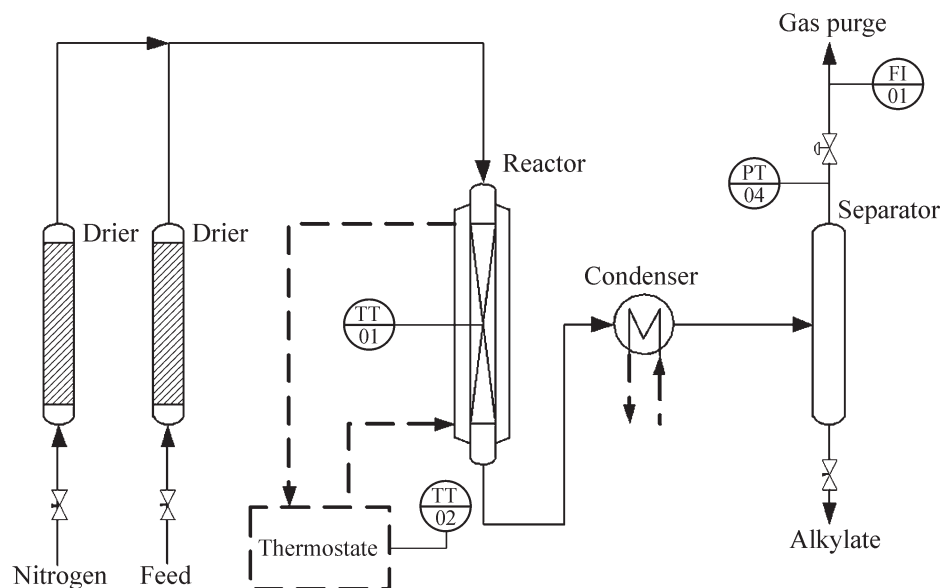
| Sample         | Description                                                                                                          |
|----------------|----------------------------------------------------------------------------------------------------------------------|
| SZ             | Sulfated zirconium hydroxide calcined at 700°C                                                                       |
| H-Beta         | Starting H-Beta zeolite calcined at 700°C                                                                            |
| B4, B8, B16    | Samples containing 4, 8, and 16 wt % zirconium dioxide, supported by H-Beta zeolite and calcined at 700°C            |
| B4S, B8S, B16S | Samples containing 4, 8, and 16 wt % zirconium dioxide, supported by H-Beta zeolite, sulfated, and calcined at 700°C |

adsorption was performed at a temperature of 77.3 K. Adsorption-desorption isotherms were recorded at 27 points; for the adsorption isotherm, the specific surface area was calculated by multiple-point Brunauer–Emmett–Teller (BET) equation. The volume of mesopores was determined by the Barrett–Joyner–Halenda (BJH) method from the desorption branch of the isotherm, the volume of micropores was determined by the Dubinin method.

An elemental no-reference semi-quantitative analysis of the catalyst samples was made by the method of energy-dispersive X-ray fluorescence spectroscopy (EDX) on a Shimadzu-8000 instrument. The analysis was performed in air, the spectrometer was equipped with a rhodium anode with 50 kV and 137  $\mu$ A, the concentrations were calculated by the no-reference method of fundamental parameters.

The catalytic activity was determined in a reactor with fixed catalyst bed (Fig. 1). A catalyst (15 cm<sup>3</sup>) was placed in the reactor, the pressure in the system was maintained at 13 bar with nitrogen, and the bed temperature was maintained at 80°C with thermostated circulated water. As the starting substance served a 20 : 1 mixture of isobutane with isobutylene, the raw material was delivered at a mass rate of 0.35 h<sup>-1</sup> (in terms of olefin). After 30 min from the beginning of the reaction, the collected alkylate was analyzed with a Shimadzu GC-2010-plus gas chromatograph equipped with a Petrocol DH column 100  $\times$  0.25 capillary column.

**XRD and EDX analyses.** The diffraction patterns of the samples are shown in Fig. 2. For each XRD pattern, the signal associated with the presence of the amorphous phase was separated from the initial spectrum.

**Fig. 1.** Schematic of the reactor installation.

**Table 2.** Degree of crystallinity of catalyst samples

| Sample | Crystallinity, % |
|--------|------------------|
| H-Beta | 71               |
| B4     | 59               |
| B8     | 60               |
| B16    | 49               |
| B4S    | 60               |
| B8S    | 56               |
| B16S   | 49               |

The degree of crystallinity was calculated by

$$\text{Cryst} = \frac{A_{\text{total}} - A_{\text{halo}}}{A_{\text{total}}} \times 100\%, \quad (1)$$

where  $A_{\text{total}}$  is the area under the curve in the spectrum, and  $A_{\text{halo}}$  is the area under the curve corresponding to the amorphous phase of a sample.

The results of this determination are listed in Table 2.

Tetragonal or monoclinic modifications of zirconium dioxide were expected to be observed for supported sulfated and sulfate-free catalyst samples. However, according to XRD data, no reflections characteristic of these modifications at angles  $2\theta = 27\text{--}33^\circ$  were observed [9]. Instead, the peak intensities became lower

with increasing content of zirconium dioxide, which is accounted for by the screening of X-rays and distortion of their diffraction pattern, caused by the presence of the supported zirconium dioxide.

It should be noted that the structure of the zeolites may change under alkaline (in deposition of zirconium dioxide) and acid conditions (in sulfation of the supported zirconium hydroxide) due to the partial dissolution of silicon dioxide or aluminum oxide forming the lattice of the zeolite. Based on published data, we can assume that the crystal structure of the starting zeolite was preserved after all the treatments, as, e.g., it was noted in [10] according to XRD data, where a decrease in the intensity of reflections in diffraction patterns of a coked catalyst based on H-Beta zeolite was observed, with its structure preserved.

Elemental analysis shows that all the supported samples contain S and Zr elements (Table 3). The presence of sulfur in calcined samples indicates that an active component is formed as sulfo groups bound to the surface of zirconium dioxide, which are preserved after the thermal treatments of the samples.

**Specific surface area and porosity.** The isotherms of low-temperature adsorption-desorption of nitrogen are shown in Fig. 3 for catalysts based on H-Beta (the range of relative adsorbate pressures of 0.3–1 is distinguished). The specific surface area and the mesopore volume, calculated by BET and BJH methods, and the micropore volume found by the Dubinin method are presented in Table 4.

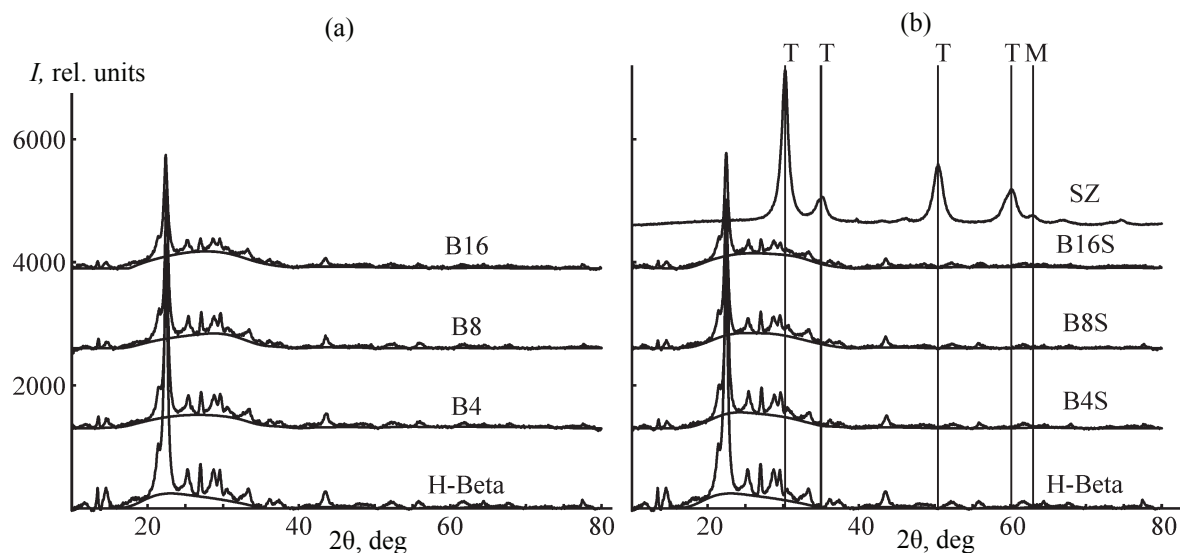


**Fig. 2.** XRD patterns of samples calcined at 700°C: sulfated zirconium dioxide, zirconium dioxide supported by H-Beta zeolite, and sulfated zirconium dioxide supported by H-Beta zeolite. (*I*) Intensity and ( $2\theta$ ) Bragg angle. The designations T and M correspond to the positions of the reflections associated with the tetragonal and monoclinic crystalline modifications of zirconium dioxide.

**Table 3.** EDX data for samples of sulfated zirconium dioxide supported by H-Beta zeolite

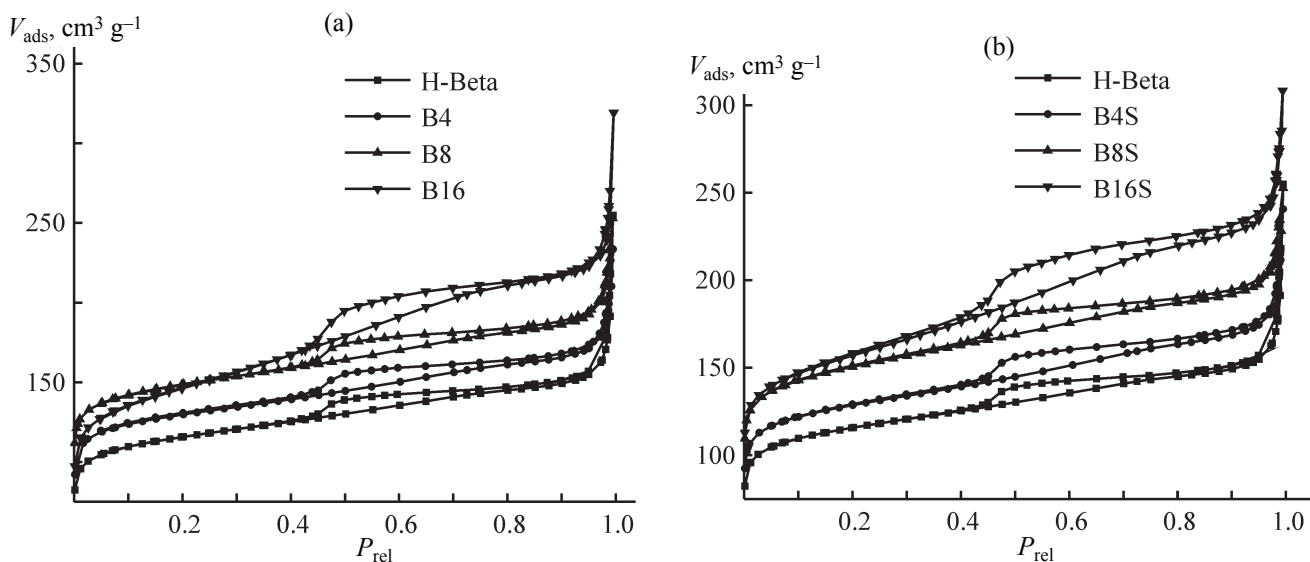
| Sample | Concentration of elements in terms of the indicated oxides, wt % |                                |                  |                 |
|--------|------------------------------------------------------------------|--------------------------------|------------------|-----------------|
|        | SiO <sub>2</sub>                                                 | Al <sub>2</sub> O <sub>3</sub> | ZrO <sub>2</sub> | SO <sub>3</sub> |
| B4S    | 92.2                                                             | 3.7                            | 1.7              | 2.4             |
| B8S    | 90.1                                                             | 3.4                            | 2.7              | 3.8             |
| B16S   | 89.1                                                             | 3.4                            | 3.3              | 4.3             |

**Table 4.** Texture properties of catalysts

| Sample | Specific surface area by BET, m <sup>2</sup> g <sup>-1</sup> | Mesopore volume                 | Micropore volume |
|--------|--------------------------------------------------------------|---------------------------------|------------------|
|        |                                                              | cm <sup>3</sup> g <sup>-1</sup> |                  |
| H-Beta | 600                                                          | 0.24                            | 0.29             |
| B4     | 577                                                          | 0.18                            | 0.28             |
| B8     | 569                                                          | 0.19                            | 0.28             |
| B16    | 539                                                          | 0.31                            | 0.31             |
| B4S    | 568                                                          | 0.19                            | 0.28             |
| B8S    | 568                                                          | 0.18                            | 0.28             |
| B16S   | 504                                                          | 0.27                            | 0.29             |
| SZ     | 190                                                          | 0.29                            | 0                |

The starting H-Beta zeolite has the adsorption-desorption isotherm belonging to type-IIb, with an H3 hysteresis loop [11], which is characteristic of materials constituted by aggregates (weakly bound) of lamellar

particles forming narrow pores [12]. After zirconium dioxide is deposited onto the starting zeolite, the hysteresis loop becomes wider, which indicates that the number of mesopores in the samples increases. It is

**Fig. 3.** Isotherms of low-temperature adsorption of nitrogen for supported catalyst samples. ( $V_{\text{ads}}$ ) Adsorbed volume and ( $P_{\text{rel}}$ ) relative pressure. The isotherms are shifted along the vertical axis for perception convenience.

**Table 5.** Results of IR spectroscopic analysis of the catalysts

| Sample | Brønsted centers, $\mu\text{mol g}^{-1}$ |                 |        |       | Lewis centers, $\mu\text{mol g}^{-1}$ |        |        |       | $B_{\text{strong}}/\Sigma L$ |
|--------|------------------------------------------|-----------------|--------|-------|---------------------------------------|--------|--------|-------|------------------------------|
|        | weak                                     | medium-strength | strong | total | weak                                  | medium | strong | total |                              |
| H-Beta | 31                                       | 13              | 138    | 182   | 246                                   | 99     | 52     | 397   | 0.35                         |
| B4S    | 46                                       | 33              | 199    | 278   | 187                                   | 66     | 26     | 280   | 0.71                         |
| B8S    | 49                                       | 22              | 119    | 190   | 144                                   | 43     | 20     | 208   | 0.57                         |
| B16S   | 39                                       | 27              | 71     | 137   | 115                                   | 29     | 9      | 153   | 0.46                         |
| SZ     | 9                                        | 14              | 108    | 141   | 19                                    | 12     | 5      | 36    | 3.0                          |

possible to determine whether or not zirconium dioxide blocks pores of the starting zeolite from the change in the relative pressure of the adsorbate, at which the adsorption and desorption branches of an isotherm converge. For

example, the adsorbate present in a partly blocked pore can leave it only if the relative pressure of the adsorbate is lowered. In the present study, the adsorption and desorption branches of isotherms converge at the same

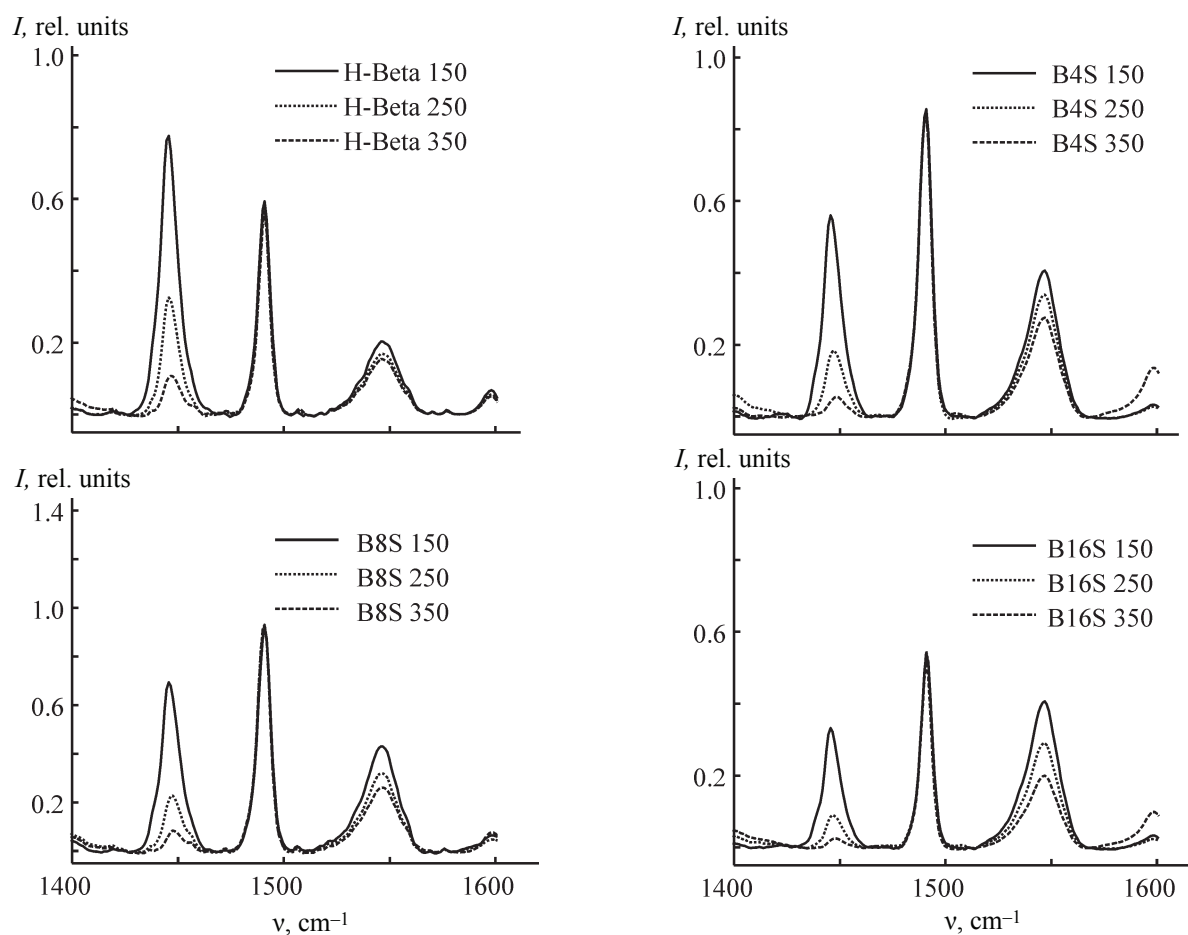


**Fig. 4.** IR spectra of chemisorbed pyridine on the surface of H-Beta, B4S, B8S, and B16S catalysts after the desorption of pyridine at 150, 250, and 350°C. (*I*) Intensity and (*v*) wave number.



relative pressure; thus, the porous structure of the starting zeolite is not distorted.

The specific surface area of the samples based on H-Beta zeolite tends to decrease with increasing amount of zirconium oxide, with the volume of micropores remaining unchanged. This indicates that zirconium dioxide particles are localized in the intercrystallite space of the zeolite and they form the intrinsic porosity [13].

**Acidity.** Measurements of the acidity of the catalyst samples demonstrated that Lewis (L) and Brønsted (B) acid centers are present in the samples under study. Detailed information about their concentration is presented in Table 5. Figure 4 shows IR spectra of pyridine adsorbed on the surface of catalyst samples based on zeolite at desorption temperatures of 150, 250, 350°C. The starting sample of H-Beta zeolite shows that Lewis acid centers are predominant in number over Brønsted centers. The concentration of Brønsted acid centers (both the total concentration and that of strong acid centers) in supported catalyst samples passes through a minimum in the dependence on the content of sulfated zirconium dioxide, whereas the concentration of Lewis acid centers gradually decreases. The maximum B/L concentration ratio is observed for sample B4S. Acidity measurements demonstrated that sulfated zirconium dioxide (sample SZ) is characterized by the predominance of Brønsted acid centers over Lewis centers. Thus, the increase in the concentration of Brønsted acid centers in sample B4S suggests that the supported phase exhibits the highest activity in the given catalyst sample as compared with the rest of the supported samples.

It can be assumed that the nonlinear dependence of the concentration of acid centers of both types on the

*S, K, wt %*

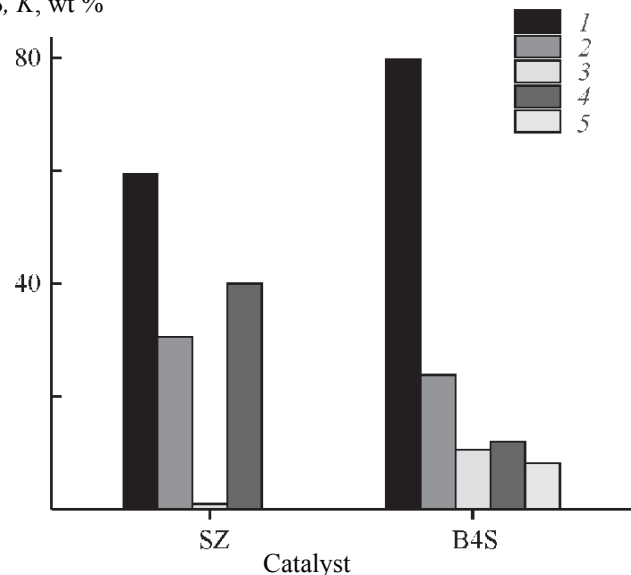


**Fig. 5.** Results obtained when determining the selectivity *S* after 210 min of the reaction (1) with respect to  $C_8$  hydrocarbons; (3) with respect to trimethylpentanes; (4) with respect to  $C_{9+}$  hydrocarbons; (5) with respect to  $C_5$ – $C_7$  hydrocarbons; and (2) conversion *K* of isobutylene.

amount of the supported phase may be due both to the inhomogeneous distribution of sulfuric acid throughout the supported catalyst sample in the sulfation stage (different degrees of sulfation due to the falling of a part of sulfuric acid onto the zeolite substrate) and also to the possible differences in crystallization and distribution of the supported component in the synthesis stage.

**Alkylation of isobutane with isobutylene.** The activity was experimentally determined for each catalyst sample, the reaction product (alkylate) was sampled in 30 min. The distribution of hydrocarbons in the alkylate is

**Table 6.** Data on the catalyst activity after 30 min of the reaction

| Catalyst    | Group composition of the alkylate, wt % |       |          | Share of 2,2,4-TMP among $C_8$ hydrocarbons, wt % | Conversion |
|-------------|-----------------------------------------|-------|----------|---------------------------------------------------|------------|
|             | $C_5$ – $C_7$                           | $C_8$ | $C_{9+}$ |                                                   |            |
| H-Beta      | 2                                       | 1     | 97       | –                                                 | 44         |
| B4S         | 11                                      | 80    | 9        | 23.5                                              | 62         |
| B8S         | 11                                      | 21    | 68       | 24.2                                              | 51         |
| B16S        | 0                                       | 1     | 99       | –                                                 | 47         |
| SZ          | 4                                       | 84    | 12       | 10.4                                              | 60         |
| SZ + H-Beta | 18                                      | 60    | 23       | –                                                 | 69         |

presented in Table 6. Because just the strong Brønsted acid centers are active in the alkylation reaction [14], the selectivity with respect to the target products grows as their fraction in the samples increases. The maximum selectivity with respect to  $C_8$  was reached when sample B4S was tested. Bulk sulfated zirconium dioxide SZ demonstrated a low selectivity with respect to  $C_{9+}$  hydrocarbons and a high yield of  $C_8$  hydrocarbons. Nevertheless, the share of the main component 2,2,4-trimethylpentane (2,2,4-TMP) among  $C_8$  hydrocarbons indicates that predominantly polymerization and cracking of oligomeric products occur on the catalyst. According to the results of these tests, the conversion of isobutylene decreases with increasing amount of  $C_{9+}$  hydrocarbons in the reaction product, which evidences that the catalysts under study are poisoned by oligomeric by-products.

A 1 : 1 mechanical mixture of two active components (designated as SZ + H-Beta), H-Beta zeolite and bulk sulfated zirconium dioxide, was molded with a Pural SB binder. The composition of the alkylate obtained with this catalyst demonstrates simultaneously a high yield of  $C_8$  and  $C_{9+}$  hydrocarbons. No high concentration of heavy hydrocarbons was observed, as, e.g., in the case for the supported catalyst B4S. Thus, it can be concluded that the supported catalyst samples possess a unique activity and selectivity, with a certain synergism exhibited between the active components in the formulation. These results are promising and demonstrate the advantage of new supported catalysts, which combine different in nature and mutual arrangement types of acid centers in the same hybrid material.

The stability of the catalysts was compared for B4S and SZ samples (Fig. 5). Analysis of the reaction products formed in 210 min shows that SZ sample demonstrates an isobutylene conversion exceeding that for the supported catalyst sample B4S. Nevertheless, the selectivity of B4S sample with respect to the key products,  $C_8$  hydrocarbons, including trimethylpentanes, after 210 min of the reaction is higher, which is an advantage of the supported catalyst over its analog.

It has been shown [15] that the effective removal of carbon deposits and primary products of the alkylation reaction from the outer surface of H-Beta zeolite and pore mouths makes slower its deactivation rate. It was shown in [16] that the deactivation of H-Beta zeolite as a result of only poisoning of the acid centers occurs at its

particle size of about 14 nm. Otherwise, the deactivation mechanism includes the pore blocking by by-products formed in the reaction. Thus, it can be concluded that the higher activity and the longer service life of the supported catalyst B4S, compared with the starting zeolite, are due to the protective function of sulfated zirconium dioxide that is deposited on the surface of zeolite crystallites and precludes accumulation of by-products via cracking of oligomerization products.

## CONCLUSIONS

(1) It was shown that, when supported by H-Beta zeolite, zirconium dioxide is deposited in the intercrystallite space of the zeolite, with the structure of the starting zeolite not disturbed after the deposition and sulfation stages. The variation of the surface acidity is correlated with the amount of the deposited sulfated zirconium dioxide and has an extremum point at around 4 wt %.

(2) It was confirmed experimentally that hybrid catalysts based on H-Beta zeolite with supported sulfated zirconium dioxide (sample with 4 wt % sulfated zirconium oxide) are more stable and exhibit a higher, in the course of time, selectivity with respect to  $C_8$  hydrocarbons and trimethylpentanes, compared with bulk sulfated zirconium dioxide. Thus, the hybrid catalysts are a promising trend in the development of the industrial alkylation process.

## ACKNOWLEDGMENTS

The study was carried out under a State contract based on a grant from the Government of the Russian Federation for support of research performed under supervision of leading scientists from Russia's higher-school institutions, research institutes, and state research centers of the Russian Federation of March 19, 2014, no. 14.Z50.31.0013.

## REFERENCES

1. Vlasov, E.A., *Catal. Lett.*, 2015, vol. 145, no. 9, pp. 1651–1659.
2. Chen, A., *J. Chinese Chem. Soc.*, 2010, no. 57, pp. 820–828.
3. Busto, M., *Fuel Process. Technol.*, 2012, vol. 104, pp. 128–135.



4. Kustov, L.M., *Russ. J. Phys. Chem. A*, 2015, vol. 89, no. 11, pp. 2006–2021.
5. Gizetdinova, A., *J. Chem. Chem. Eng.*, 2014, vol. 8, no. 5, pp. 453–460.
6. US Patent 7 794 687 B2 (publ. 2010).
7. Devyatkov, S.Y., *Ind. Eng. Chem. Res.*, 2016, vol. 55, no. 23, pp. 57–64
8. Emeis, C.A., *J. Catal.*, 1993, vol. 14, no. 2, pp. 347–354.
9. Gauna, M.R., *Ceram. - Silik.*, 2015, vol. 50, no. 4, pp. 318–325.
10. Adebajo, M.O., *Spectrochim. Acta, Part A*, 2004, vol. 60, no. 4, pp. 791–799.
11. Qi, X., *J. Mater. Sci.*, 2008, vol. 43, no. 16, pp. 5626–5633.
12. Sing, K.S.W., *Assessment of Mesoporosity*, Elsevier, 2014.
13. Ye, F., *Catal. Commun.*, 2009, vol. 10, pp. 2056–2059.
14. Feller, A., *J. Catal.*, 2003, vol. 216, nos. 1–2, pp. 313–323.
15. Salinas, A.L., *Appl. Catal., A*, 2008, vol. 336, nos. 1–2, pp. 313–323.
16. Loenders, R., *J. Catal.*, 1998, vol. 176, pp. 545–551.